



# Global Phase Portrait of a Rolling Motion of Ships Equation

Martha Álvarez-Ramírez<sup>1</sup> · Jaume Llibre<sup>2</sup>

Received: 10 August 2024 / Accepted: 17 January 2025 / Published online: 30 January 2025  
© The Author(s) 2025

## Abstract

This paper studies the global dynamics of the rolling motion of ships in random beam seas model described by the equation

$$\ddot{x} + (2\mu + \delta x^2)\dot{x} + \omega^2 x - \frac{1}{a^2}x^3 = 0,$$

where  $0 < \mu \ll 1$ ,  $0 < \delta < 1$ ,  $\omega = 1$  and  $0 < a < 3$ . We fully explain its dynamics in the Poincaré compactification of  $\mathbb{R}^2$ .

**Keywords** Poincaré compactification · Equilibrium points · Topological phase portraits

**Mathematics Subject Classification** Primary 34C05; Secondary 37C10

## 1 Introduction and Statement of Results

The study of the problem of the movement of ships at sea consists of solving the equations of the dynamic equilibrium of forces and moments. Indeed, there are three possible displacement motions (sway or drift, surge and heave) that ships can undergo, as well as three angular motions (roll, yaw and pitch). Some authors have experimentally studied roll damping to visualize local flows, see for instance, [5] and [10]. Meanwhile, researchers investigated mathematical modeling of roll damping. In this work we consider a model given by a second-order ordinary nonlinear differential

This work was completed with the support of our T<sub>E</sub>X-pert.

✉ Martha Álvarez-Ramírez  
mar@xanum.uam.mx

Jaume Llibre  
jaume.llibre@uab.cat

<sup>1</sup> Departamento de Matemáticas, Universidad Autónoma Metropolitana - Iztapalapa, 09310 Mexico City, Mexico

<sup>2</sup> Departament de Matemàtiques, Universitat Autònoma de Barcelona, Bellaterra, 08193 Barcelona, Catalonia, Spain

equation with cubic damping moment and without forcing, namely

$$\ddot{x} + (2\mu + \delta x^2)\dot{x} + \omega^2 x - \frac{1}{a^2}x^3 = 0, \quad (1.1)$$

where the dot denotes  $d/dt$ ,  $\omega$  is the angle frequency without dimensions,  $-1/a^2$  is the force of the nonlinear coefficient,  $\mu$  is the dimensionless damping coefficient, and  $\delta$  is the quadratic viscous damping coefficient. For more studies related with this equation, including the importance of its study, we refer the readers, in among, to [3, 5]. Particularly, in these works the authors used ultraspherical wavelets to obtain a numerical solution of equation (1.1).

Next, we write the equation (1.1) as a system of first order differential equations. Then we may write

$$\dot{x} = y, \quad \dot{y} = -(2\mu + \delta x^2)y - x + \frac{1}{a^2}x^3. \quad (1.2)$$

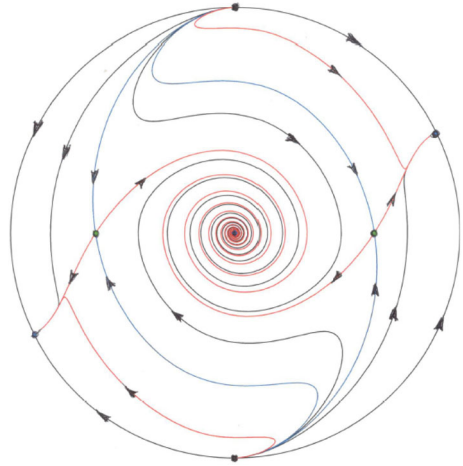
By taking the parameter values  $0 < \mu \ll 1$ ,  $0 < \delta < 1$ ,  $\omega = 1$  and  $0 < a < 3$ , we perform a global analysis of its dynamics in the Poincaré disc. We have consider these values of the parameters because experimental values for the present parameters in equation (1.2) are  $\mu = 0.005$ ,  $\delta = 0.1$ ,  $\omega = 1$ ,  $1/a^2 = 0.2$ , i.e.  $a = \sqrt{5}$ , see [5].

The Poincaré disc  $\mathbb{D}$  is defined as the closed unit disc, where its interior is identified with the Euclidean plane  $\mathbb{R}^2$ . The boundary of  $\mathbb{D}$ , which is the unit circle  $\mathbb{S}^1$ , corresponds to the point at infinity in  $\mathbb{R}^2$ . In this context, points within the interior of  $\mathbb{D}$  represent finite points in the plane, while points approaching the boundary of  $\mathbb{D}$  represent directions of approach to infinity in  $\mathbb{R}^2$ . This identification allows us to study the geometry of  $\mathbb{R}^2$  using the properties of the disc and its boundary. Moreover, a polynomial differential system defined in  $\mathbb{R}^2$  can be analytically extended to the entire Poincaré disc  $\mathbb{D}$ . This extension facilitates the analysis of orbit behavior as they approach or recede from infinity. Detailed information on Poincaré compactification is provided in Appendix A. Analyzing phase portraits of polynomial differential systems using the Poincaré disc is a well-established method; see, for example, [6].

We would like to remind readers that the phase portrait of a polynomial differential system on the Poincaré disc is constructed by decomposing the disc into the union of the system's orbits. This process involves identifying equilibrium points, analyzing the behavior of orbits in their vicinity, and investigating the existence of periodic orbits. The phase portrait thereby encapsulates all the qualitative properties of the system's orbits, including their starting and ending points. To determine the phase portrait, it suffices to analyze the configuration of the system's separatrices. Further details can be found in Appendix B. Additionally, Appendix C explains the blow-up technique used to desingularize degenerate singular points in the planar vector fields studied in this work.

Since the system (1.2) is invariant under the symmetry  $S : (x, y) \rightarrow (-x, -y)$ , it follows that if  $\gamma(t) = (x(t), y(t))$  is a solution of the system, then  $S(\gamma(t)) = (-x(t), -y(t))$  is also a solution. In other words, the solutions are symmetric with respect to the origin of coordinates.

**Fig. 1** The phase portrait in the Poincaré disc of the differential system (1.2) with  $0 < \mu \ll 1$ ,  $0 < \delta < 1$ ,  $\omega = 1$  and  $0 < a < 3$



We summarize our main result in the next theorem.

**Theorem 1.1** *The phase portrait in the Poincaré disc of the system (1.2) with  $0 < \mu \ll 1$ ,  $0 < \delta < 1$ ,  $\omega = 1$  and  $0 < a < 3$  is topologically equivalent to the one in Fig. 1.*

From Fig. 1 we conclude that if and only if the initial conditions of the boat are in the basin of attraction of the strong focus, localized at the origin of coordinates, the boat has no problems, otherwise the boat will have several problems, because from the phase portrait of Fig. 1 the variable  $x$  will tend to infinity in forward time.

The phase portrait of Fig. 1 has 19 separatrices and 6 canonical regions, for precise definitions of separatrices and canonical regions see the Appendix B.

## 2 The Poincaré disc with the Global Phase Portrait

In this section, we start by examining the finite equilibrium points of system (1.2), followed by an analysis of the infinite equilibrium points. Finally, we present the global phase portraits of system (1.2).

### 2.1 The Finite Equilibrium Points of System (1.2)

A direct calculation shows that system (1.2) has the following finite equilibrium points when  $a \neq 0$ ,

$$p_0 = (0, 0), \quad p_1 = (-a, 0), \quad p_2 = (a, 0). \quad (2.1)$$

The eigenvalues of the point  $p_0$  are  $-\mu \pm \sqrt{\mu^2 - 1} \in \mathbb{C}$ , since  $0 < \mu \ll 1$ . Thus we have that  $p_0$  is a hyperbolic stable focus, see Theorem 2.15 of [4]. The points  $p_1$  and  $p_2$  have eigenvalues

$$\frac{1}{2} \left( -a^2\delta - 2\mu + \sqrt{8 + (a^2\delta + 2\mu)^2} \right) > 0,$$

and

$$\frac{1}{2} \left( -a^2\delta - 2\mu - \sqrt{8 + (a^2\delta + 2\mu)^2} \right) < 0.$$

Then  $p_1$  and  $p_2$  are hyperbolic saddles.

## 2.2 Infinite Equilibrium Points of System (1.2)

To fully characterize the global phase portrait of system (1.2) within the Poincaré disc, we need to examine its infinite equilibrium points (see Appendix A).

In the local chart  $U_1$  the system (1.2) is transformed into

$$\begin{aligned} \dot{u} &= \frac{1}{a^2} - \delta u - v^2 - 2\mu uv^2 - u^2 v^2, \\ \dot{v} &= -uv^3. \end{aligned} \quad (2.2)$$

The point  $p = (1/(a^2\delta), 0)$  is the only infinite equilibrium point in the chart  $U_1$ . Moreover, the linearization of (2.2) at  $p$  yields eigenvalues 0 and  $-\delta$ , then  $p$  is a semi-hyperbolic equilibrium point. So we shall apply Theorem 2.19 of [4] for determining its local phase portrait. First we bring the equilibrium  $p$  to origin of coordinates. Then, the differential equation becomes

$$\begin{aligned} \dot{u}_1 &= -\delta u_1 - \left( 1 + \frac{1}{a^4\delta^2} + \frac{2\mu}{a^2\delta} \right) v_1^2 - 2 \left( \frac{1}{a^2\delta} + \mu \right) u_1 v_1^2 - u_1^2 v_1^2, \\ \dot{v}_1 &= -\frac{1}{a^2\delta} v_1^3 - u_1 v_1^3. \end{aligned} \quad (2.3)$$

To apply Theorem 2.19 we need that the coefficient of the variable  $u_1$  in  $\dot{u}_1$  be positive, so we change the sign in the differential system (2.3):

$$\begin{aligned} \dot{u}_1 &= \delta u_1 + \left( 1 + \frac{1}{a^4\delta^2} + \frac{2\mu}{a^2\delta} \right) v_1^2 + 2 \left( \mu + \frac{1}{a^2\delta} \right) u_1 v_1^2 + u_1^2 v_1^2, \\ \dot{v}_1 &= \frac{1}{a^2\delta} v_1^3 + u_1 v_1^3. \end{aligned} \quad (2.4)$$

According to Theorem 2.19 of [4], the infinite equilibrium point  $p$  of system (2.4) is a semi-hyperbolic unstable node, because  $1/(a^2\delta) > 0$ . However, due to the change of time applied in this theorem, the point  $p$  in the local chart  $U_1$  becomes a semi-hyperbolic stable node.

We still need to verify whether the origin of the  $U_2$  local chart is another infinite equilibrium point. In the chart  $U_2$  the system (1.2) becomes

$$\begin{aligned} \dot{u} &= v^2 + \delta u^3 + 2\mu uv^2 - \frac{1}{a^2} u^4 + u^2 v^2, \\ \dot{v} &= 2\mu v^3 + \delta u^2 v + uv^3 - \frac{1}{a^2} u^3 v. \end{aligned} \quad (2.5)$$

Therefore, the point  $(0, 0)$  on the chart  $U_2$  is an infinite equilibrium point. Since the linear part of equation (2.5) is the identically zero matrix, determining the local phase portrait at the equilibrium point  $(0, 0)$  requires a change of variables known as blow-ups (see [1], or the Appendix C). The characteristic direction at the equilibrium point  $(0, 0)$  is given by  $v^3 = 0$ . However, since the direction  $u = 0$  is not a characteristic direction (for more details on characteristic directions at an equilibrium point, see [2]), we will perform a vertical blow-up using the change of variables  $u = u_1$  and  $v = u_1 v_1$ . Additionally, we scale the time variable of the system by  $dt_1 = u_1 dt$ . Thus, system (2.5) can be rewritten as:

$$\begin{aligned}\dot{u}_1 &= \frac{u_1}{a^2} \left( a^2 \delta u_1 - u_1^2 + a^2 v_1^2 + 2a^2 \mu u_1 v_1^2 + a^2 u_1^2 v_1^2 \right), \\ \dot{v}_1 &= -v_1^3.\end{aligned}\quad (2.6)$$

Here the dot denotes derivative  $d/dt_1$ . Notice that the only equilibrium point on the line  $u_1 = 0$  is at  $(0, 0)$ , which is also linearly zero. For this differential system, the characteristic directions at the equilibrium point  $(0, 0)$  are given by  $u_1^2 v_1 = 0$ , indicating that  $u_1 = 0$  is a characteristic direction. However, to retain all relevant information during a subsequent vertical blow-up, it is crucial to ensure that the direction  $u_1 = 0$  is not a characteristic direction at the origin of system (2.6). First, we perform the twist  $(u_1, v_1) = (u_2 - v_2, v_2)$ . In the new variables  $(u_2, v_2)$ , the differential system (2.6) is then expressed as

$$\begin{aligned}\dot{u}_2 &= \delta u_2^2 - 2\delta u_2 v_2 + \delta v_2^2 - \frac{1}{a^2} u_2^3 + \frac{3}{a^2} u_2^2 v_2 + \left(1 - \frac{3}{a^2}\right) u_2 v_2^2 + \left(\frac{1}{a^2} - 2\right) v_2^3 \\ &\quad + 2\mu u_2^2 v_2^2 - 4\mu u_2 v_2^3 + 2\mu v_2^4 - 3u_2^2 v_2^3 + 3u_2 v_2^4 + u_2^3 v_2^2 - v_2^5, \\ \dot{v}_2 &= -v_2^3.\end{aligned}\quad (2.7)$$

At this stage, we make a second blow-up  $(u_2, v_2) = (u_3, u_3 v_3)$  and another change to the time scale  $dt_2 = u_3 dt_1$ , keeping the dot for the derivative with respect to the new time  $t_2$ . Then we get the following system

$$\begin{aligned}\dot{u}_3 &= -\frac{1}{a^2} u_3 \left[ -a^2 \delta + u_3 + 2a^2 \delta v_3 - 3u_3 v_3 - a^2 \delta v_3^2 + (3 - a^2) u_3 v_3^2 \right. \\ &\quad \left. - 2a^2 \mu u_3^2 v_3^2 + (-1 + 2a^2) u_3 v_3^3 - a^2 u_3^3 v_3^2 + 4a^2 \mu u_3^2 v_3^3 \right. \\ &\quad \left. + 3a^2 u_3^3 v_3^3 - 2a^2 \mu u_3^2 v_3^4 - 3a^2 u_3^3 v_3^4 + a^2 u_3^3 v_3^5 \right], \\ \dot{v}_3 &= \frac{1}{a^2} v_3 (v_3 - 1) \left[ a^2 \delta - u_3 - a^2 \delta v_3 + 2u_3 v_3 + (2a^2 - 1) u_3 v_3^2 \right. \\ &\quad \left. + 2a^2 \mu u_3^2 v_3^2 + a^2 u_3^3 v_3^2 - 2a^2 \mu u_3^2 v_3^3 - 2a^2 u_3^3 v_3^3 + a^2 u_3^3 v_3^4 \right].\end{aligned}\quad (2.8)$$

It is not difficult to check that the equilibrium points of system (2.8) on the line  $u_3 = 0$  are  $(0, 0)$  and  $(0, 1)$ . The eigenvalues of the Jacobian matrix of (2.8) at the origin are  $\delta$  and  $-\delta$  indicating that  $(0, 0)$  is a hyperbolic saddle point. However, the Jacobian matrix of system (2.8) at  $(0, 1)$  is the zero matrix. Consequently, we need to

use the blow-up technique to analyze the local phase portrait at this equilibrium point. To apply this technique, we first bring the point  $(0, 1)$  to the origin by introducing new coordinates. Let  $(u_3, v_3) = (u_4, 1 + v_4)$ ; in these coordinates, system (2.8) takes the following form:

$$\begin{aligned}\dot{u}_4 &= -\frac{1}{a^2}u_4 \left[ a^2u_4 + 4a^2u_4v_4 - a^2v_4^2 + 5a^2u_4v_4^2 + (-1 + 2a^2)u_4v_4^3 - 2a^2\mu u_4^2v_4^2 \right. \\ &\quad \left. - 4a^2\mu u_4^2v_4^3 + a^2u_4^3v_4^3 - 2a^2\mu u_4^2v_4^4 + 2a^2u_4^3v_4^4 + a^2u_4^3v_4^5 \right], \\ \dot{v}_4 &= \frac{1}{a^2}v_4(1 + v_4) \left[ 2a^2u_4 - a^2\delta v_4 + 4a^2u_4v_4 - 2a^2\mu u_4^2v_4 \right. \\ &\quad \left. + (2a^2 - 1)u_4v_4^2 - 4a^2\mu u_4^2v_4^2 + a^2u_4^3v_4^2 - 2a^2u_4^2v_4^3 + 2a^2u_4^3v_4^3 + a^2u_4^3v_4^4 \right].\end{aligned}\quad (2.9)$$

At  $(0, 0)$  the characteristic directions of the system (2.9) are given by  $u_4^2v_4 = 0$ . Since  $u_4 = 0$  corresponds to a characteristic direction at the origin of (2.9), we first need to move  $u_4 = 0 - u_5 = v_5$ , before performing a vertical blow-up. This can be achieved by the twist  $(u_4, v_4) = (u_5 - v_5, v_5)$ . It is straightforward to see that, in these new variables, system (2.9) takes the form:

$$\begin{aligned}\dot{u}_5 &= -u_5^2 + 4u_5v_5 - (3 + \delta)v_5^2 - 4u_5^2v_5 + (14 + \delta)u_5v_5^2 - (10 + 2\delta)v_5^3 \\ &\quad + (16 - \frac{1}{a^2} + 4\mu)u_5v_5^3 - (5 + 2\mu)u_5^2v_5^2 - \left(11 + \frac{1}{a^2} + 2\mu\right)v_5^4 \\ &\quad + 2\mu u_5^3v_5^2 + \left(-2 + \frac{1}{a^2} - 12\mu\right)u_5^2v_5^3 + \left(6 - \frac{3}{a^2} + 18\mu\right)u_5v_5^4 \\ &\quad + \left(-4 + \frac{2}{a^2} - 8\mu\right)v_5^5 + (1 + 4\mu)u_5^3v_5^3 - (3 + 18\mu)u_5^2v_5^4 + (3 + 24\mu)u_5v_5^5 \\ &\quad - (1 + 10\mu)v_5^6 - u_5^4v_5^3 + (7 + 2\mu)u_5^3v_5^4 - (15 + 8\mu)u_5^2v_5^5 + (13 + 10\mu)u_5v_5^6 \\ &\quad - 4(1 + \mu)v_5^7 + 11u_5^3v_5^5 - 21u_5^2v_5^6 + 17u_5v_5^7 - 5v_5^8 - u_5^4v_5^5 + 5u_5^3v_5^6 - 9u_5^2v_5^7 \\ &\quad + 7u_5v_5^8 - 2v_5^9, \\ \dot{v}_5 &= 2u_5v_5 - (2 + \delta)v_5^2 + 6u_5v_5^2 - (6 + \delta)v_5^3 - 2\mu u_5^2v_5^2 + \left(6 - \frac{1}{a^2} + 4\mu\right)u_5v_5^3 \\ &\quad + \left(-6 + \frac{1}{a^2} - 2\mu\right)v_5^4 - 6\mu u_5^2v_5^3 + \left(2 - \frac{1}{a^2} + 12\mu\right)u_5v_5^4 + \left(-2 + \frac{1}{a^2} - 6\mu\right)v_5^5 \\ &\quad + u_5^3v_5^3 - (3 + 6\mu)u_5^2v_5^4 + (3 + 12\mu)u_5v_5^5 - (1 + 6\mu)v_5^6 + 3u_5^3v_5^4 \\ &\quad - (9 + 2\mu)u_5^2v_5^5 + (9 + 4\mu)u_5v_5^6 - (3 + 2\mu)v_5^7 + 3u_5^3v_5^5 - 9u_5^2v_5^6 + 9u_5v_5^7 \\ &\quad - 3v_5^8 + u_5^3v_5^6 - 3u_5^2v_5^7 + 3u_5v_5^8 - v_5^9.\end{aligned}\quad (2.10)$$

Now we perform the vertical blow-up given by the transformation  $(u_5, v_5) \rightarrow (u_6, u_6v_6)$ , and we also scale the time variable of the system by  $dt_3 = u_6dt_2$ . The equations become

$$\dot{u}_6 = -\frac{1}{a^2}u_6 \left[ a^2 - 4a^2v_6 + 4a^2u_6v_6 + a^2(3 + \delta)v_6^2 - a^2(14 + \delta)u_6v_6^2 + a^2(5 + 2\mu)u_6^2v_6^2 \right]$$

$$\begin{aligned}
& + 2a^2(5 + \delta)u_6v_6^3 - 2a^2\mu u_6^3v_6^2 + (1 - 16a^2 - 4a^2\mu)u_6^2v_6^3 - a^2(1 - 4\mu)u_6^4v_6^3 \\
& + (3 - 6a^2 - 18a^2\mu)u_6^3v_6^4 + a^2u_6^5v_6^3 + (3a^2 + 18a^2\mu)u_6^4v_6^4 \\
& + (-2 + 4a^2 + 8a^2\mu)u_6^3v_6^5 - a^2(7 + 2\mu)u_6^5v_6^4 - 3a^2(1 + 8\mu)u_6^4v_6^5 + 2a^2u_6^6v_6^4 \\
& + a^2(15 + 8\mu)u_6^5v_6^5 + a^2(1 + 10\mu)u_6^4v_6^6 - 11a^2u_6^6v_6^5 + a^2u_6^7v_6^5 + 21a^2u_6^6v_6^6 \\
& + 4a^2(1 - \mu)u_6^5v_6^7 - 5a^2u_6^7v_6^6 - 17a^2u_6^6v_6^7 + 9a^2u_6^7v_6^7 + 5a^2u_6^6v_6^8 \\
& - 7a^2u_6^7v_6^8 + 2a^2u_6^7v_6^9 \Big], \\
\dot{v}_6 = & \frac{1}{a^2}v_6(v_6 - 1) \Big[ -3a^2 + a^2(3 + \delta)v_6 - 10a^2u_6v_6 + 2a^2\mu u_6^2v_6 \\
& + a^2(10 + 2\delta)u_6v_6^2(1 - 11a^2 - 4a^2\mu)u_6^2v_6^2 + 8a^2\mu u_6^3v_6^2 + (-1 + 11a^2 + 2a^2\mu)u_6^2v_6^3 \\
& + (2 - 4a^2 - 16a^2\mu)u_6^3v_6^3 - a^2u_6^4v_6^2 + a^2(3 + 10\mu)u_6^4v_6^3 \\
& + (-2 + 4a^2 + 8a^2\mu)u_6^3v_6^4 - 4a^2u_6^5v_6^3 - a^2(3 + 20\mu)u_6^4v_6^4 + 4a^2(3 + \mu)u_6^5v_6^4 \\
& + a^2(1 + 10\mu)u_6^4v_6^5 - 4a^2(3 + 2\mu)u_6^5v_6^5 - 5a^2u_6^6v_6^4 + 15a^2u_6^6v_6^5 \\
& + 4a^2(1 + \mu)u_6^5v_6^6 - 2a^2u_6^7v_6^5 - 15a^2u_6^6v_6^6 - 6a^2u_6^7v_6^7 \\
& + 6a^2u_6^7v_6^6 + 2a^2u_6^7v_6^8 \Big], \tag{2.11}
\end{aligned}$$

where  $\cdot = d/dt_3$ .

The equilibrium points of system (2.2) on the line  $u_6 = 0$  are  $(0, 0)$ ,  $(0, 1)$ , and  $\left(0, \frac{3}{3+\delta}\right)$ . The eigenvalues of the Jacobian matrix at  $(0, 0)$  are  $-1$  and  $3$ , while at  $(0, 1)$ , they are  $\delta$  and  $-\delta$ . Consequently, both  $(0, 0)$  and  $(0, 1)$  are hyperbolic saddles. In contrast, the eigenvalues of the linearized system at  $\left(0, \frac{3}{3+\delta}\right)$  are  $-\frac{\delta}{3+\delta} < 0$  and  $-\frac{3\delta}{3+\delta} < 0$ , indicating that it is a hyperbolic stable node.

Since the desingularization process on  $U_2$  is complete, we will do the blow down to obtain the phase portrait at the origin of the chart  $U_2$ .

- After performing the third blow-up, we obtain three equilibrium points along the line  $u_6 = 0$ . Consequently, in the neighborhood of  $u_6 = 0$ , the phase portrait of system (2.2) is topologically equivalent to the one depicted in Fig. 2a.
- By undoing the rescaling time  $dt_3 = u_6 dt_2$  and applying the variable transformations  $u_5 = u_6$  and  $v_5 = u_6 v_6$ , the curve  $v_5 = 0$  remains invariant, while the straight lines  $v_6 = \pm 1$  disappear. Therefore, the phase portrait near the origin of system (2.10) is topologically equivalent to the one illustrated in Fig. 2b.
- Back to the plane  $(u_4, v_4)$  by reversing the twist transformation  $v_5 = u_5$ , we obtain the phase portrait of system (2.9) around the origin. This portrait is topologically equivalent to the one shown in Fig. 2c.
- By retracing the blow-up process and undoing the scale change, we obtain the local phase portrait for the line  $u_3 = 0$ , as illustrated in Fig. 2d.
- Once again we carrying out the blow-down process so that straight lines  $v_3 = 1$  disappears, and also undo the rescale time  $dt_2 = u_3 dt_1$ , we get the local phase portrait at the origin of the coordinates of the system (2.7), which is topologically equivalent to the one shown in Fig. 2e.

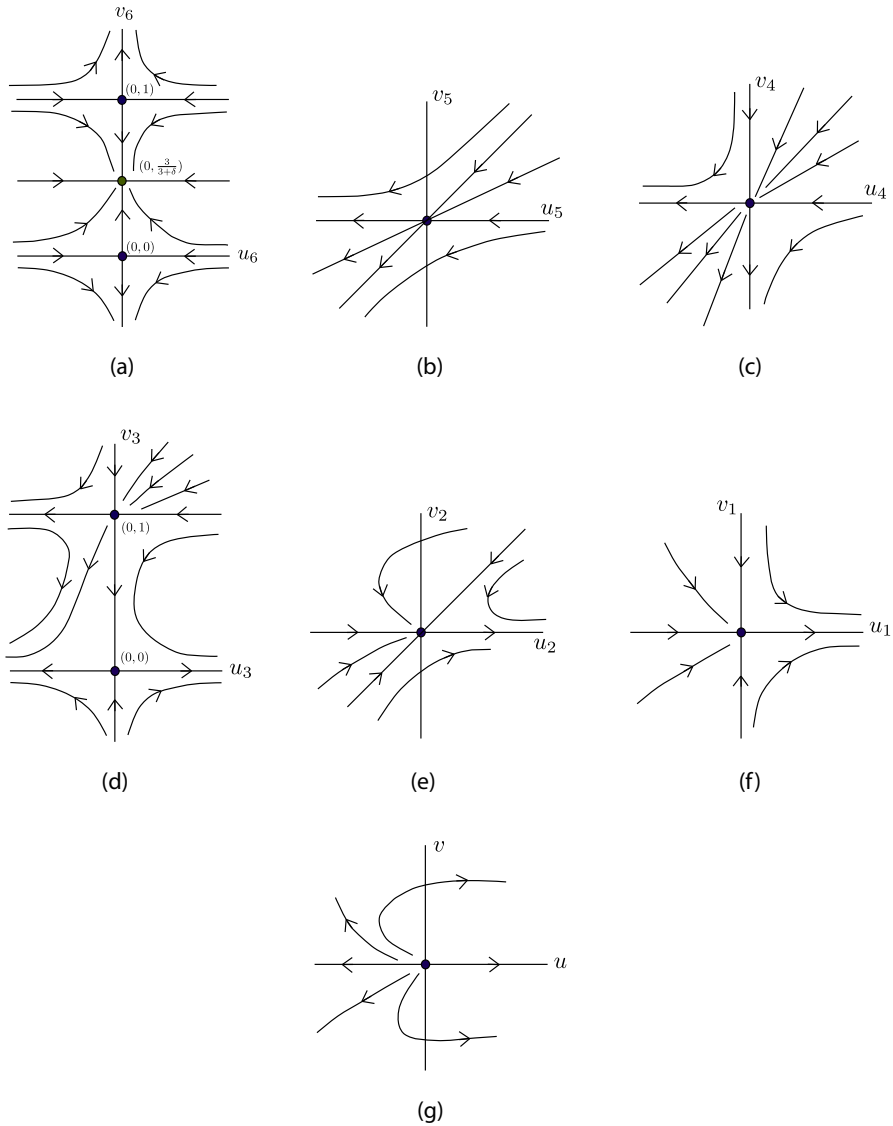


**Fig. 2** The blow-up of the equilibrium point at the origin in the local chart  $U_2$  of system (2.5)

- Going back the vertical blow-up, undoing the twist transformation, and reversing the time rescaling  $dt_1 = u_1 dt$ , the phase portrait at the origin of system (2.6) is topologically equivalent to the one depicted in Fig. 2f.
- Finally, transitioning back to system (2.5) in the local chart  $U_2$  gives us the local phase portrait near the origin. This portrait is topologically equivalent to the one depicted in Fig. 2g, indicating that the origin in the local chart  $U_2$  is an unstable node.

## 2.3 Global Phase Portrait of Systems (1.2)

For the notions of separatrix and canonical region see the section in the appendix dedicated to the topological equivalence of two polynomial vector fields.

In this section, we present the global topological portrait of system (1.2) within the Poincaré disc, utilizing the results obtained in subsections 2.1 and 2.2. We also examine the behavior of the system (1.2) along the coordinate axes, taking into account the system's symmetry with respect to the origin.

The divergence of the differential system (1.2), given by  $-2\mu - \delta x^2$ , is negative. By the Bendixson criterion (see, for instance, Theorem 7.10 in [4]), this negativity ensures that the system (1.2) cannot have periodic orbits and, consequently, no limit cycles.

By synthesizing this information, we construct the phase portrait of system (1.2) within the Poincaré disc, which is topologically equivalent to the one shown in Fig. 1.

We identify five canonical regions in the phase portrait, with the basin of attraction for the strong focus at  $(0, 0)$  corresponding to the region whose boundary contains this strong focus. Consequently, we conclude that the boat will be stable and encounter no issues if its initial conditions lie within this basin of attraction. Otherwise, it will experience various problems.

## Appendix A. Poincaré Compactification

To classify the global dynamics of a polynomial differential system, the first thing we must do is determine the finite and infinite equilibrium points in the Poincaré compactification (see Chapter 5 of [4]). The second step for determining the global dynamics in the Poincaré disc of a polynomial differential system is to characterize where start and end the separatrices.

Consider the polynomial differential systems in  $\mathbb{R}^2$  of the form

$$\dot{x} = P(x, y), \quad \dot{y} = Q(x, y), \quad (\text{A.1})$$

where the dot indicates a differentiation with respect to the time variable  $t$ . The degree of the polynomial differential system (A.1) is the maximum value  $d$  of the degrees of the polynomials  $P$  and  $Q$ . Let  $\mathcal{X} = P \frac{\partial}{\partial x} + Q \frac{\partial}{\partial y}$  be the polynomial vector field associated to system (A.1). Thus the degree of  $\mathcal{X}$  is also  $d$ . We denote by  $p(\mathcal{X})$  the analytic vector field  $\mathcal{X}$  extended to  $\mathbb{S}^2$ . In order to obtain the expression of  $p(\mathcal{X})$  we will consider the sphere as a smooth manifold.

Let  $\mathbb{R}^2$  the plane in  $\mathbb{R}^3$  given by  $(y_1, y_2, y_3) = (x_1, x_2, 1)$ . We define the Poincaré sphere as  $\mathbb{S}^2 = \{y \in \mathbb{R}^3 : y_1^2 + y_2^2 + y_3^2 = 1\}$ , this sphere is tangent to the plane  $\mathbb{R}^2$  at the point  $(0, 0, 1)$ . This sphere is divided into the northern and the southern hemispheres  $H_+ = \{y \in \mathbb{S}^2 : y_3 > 0\}$  and  $H_- = \{y \in \mathbb{S}^2 : y_3 < 0\}$ , respectively, and the equator  $\mathbb{S}^1 = \{y \in \mathbb{S}^2 : y_3 = 0\}$ .

Next, we consider the projection of the vector field  $\mathcal{X}$  to  $\mathbb{S}^2$ , where the central projection  $f : \mathbb{R}^2 \rightarrow \mathbb{S}^2$  sends every point  $x \in \mathbb{R}^2$  to the two intersection points of the straight line passing through the origin of coordinates and the point  $x$  with the sphere  $\mathbb{S}^2$ . The equator  $\mathbb{S}^1$  of the sphere is identified with the infinity of  $\mathbb{R}^2$ . Let  $Df$

the differential of  $f$ , and  $\tilde{\mathcal{X}} = Df \circ \mathcal{X}$  are two copies of the vector field  $\mathcal{X}$  defined on the sphere  $\mathbb{S}^2$  except on its equator  $\mathbb{S}^1$ .

The vector field  $\tilde{\mathcal{X}}$  can be extended analytically to a vector field on  $\mathbb{S}^2$  multiplying  $\tilde{\mathcal{X}}$  by  $y_3^d$ . Thus the new vector field  $p(\mathcal{X}) = y_3^d \tilde{\mathcal{X}}$  is defined in the whole  $\mathbb{S}^2$  and it is called the *Poincaré compactification* of the polynomial vector field  $\mathcal{X}$  on  $\mathbb{R}^2$ . The dynamics of  $\mathcal{X}$  in the neighborhood of the infinity is given by the dynamics of  $p(\mathcal{X})$  close to  $\mathbb{S}^1$ .  $\mathbb{S}^2$  is a 2-manifold, hence in order to work with the vector field  $p(\mathcal{X})$  on  $\mathbb{S}^2$ , we must have its expressions in the local charts  $(U_i, \phi_i)$  and  $(V_i, \psi_i)$ , where  $U_i = \{y \in \mathbb{S}^2 : y_i > 0\}$ ,  $V_i = \{y \in \mathbb{S}^2 : y_i < 0\}$ ,  $\phi_i : U_i \rightarrow \mathbb{R}^2$  and  $\psi_i : V_i \rightarrow \mathbb{R}^2$  for  $i = 1, 2, 3$ , with  $\phi_i(y) = -\psi_i(y) = (y_m/y_i, y_n/y_i)$  for  $m < n$  and  $m, n \neq i$ . We denote by  $(u, v)$  the local coordinates on  $U_i$  and  $V_i$ . The vector field  $p(\mathcal{X})$  in these local charts  $(U_1, \phi_1)$  and  $(U_2, \phi_1)$  are

$$\begin{aligned} \dot{u} &= v^d \left[ -uP\left(\frac{1}{v}, \frac{u}{v}\right) + Q\left(\frac{1}{v}, \frac{u}{v}\right) \right], & \dot{v} &= -v^{d+1}P\left(\frac{1}{v}, \frac{u}{v}\right) \quad \text{in } (U_1, \phi_1), \\ \dot{v} &= v^d \left[ P\left(\frac{u}{v}, \frac{1}{v}\right) - uQ\left(\frac{u}{v}, \frac{1}{v}\right) \right], & \dot{u} &= -v^{d+1}Q\left(\frac{u}{v}, \frac{1}{v}\right) \quad \text{in } (U_2, \phi_2), \end{aligned} \quad (\text{A.2})$$

respectively. The expression for the vector field  $p(\mathcal{X})$  in the local char  $(V_i, \psi_i)$  is identical to that of the local chart  $(U_i, \psi_i)$  multiplied by  $(-1)^{d-1}$  for  $i = 1, 2, 3$ . The points  $(u, v)$  of  $\mathbb{S}^1$  in any local chart with  $i = 1, 2$  have  $v = 0$ .

We note that the equator  $\mathbb{S}^1$  is invariant by the vector field  $p(\mathcal{X})$ . The *infinite equilibrium points* of  $\mathcal{X}$  are equilibrium points of  $p(\mathcal{X})$  which are in  $\mathbb{S}^1$ . Also we note that if  $y$  is an infinite equilibrium point in  $\mathbb{S}^1$ , then  $-y$  is also an infinite equilibrium point, and if the degree of the vector field is odd, these two points have the same stability or instability. This stability shifts to the contrary if the vector field's degree is even. The *Poincaré disc*, denoted by  $\mathbb{D}$ , is the projection of the closed northern hemisphere of  $\mathbb{S}^2$  on  $y_3 = 0$  by  $\pi : (y_1, y_2, y_3) \mapsto (y_1, y_2)$ .

Since the orbits of  $\mathbb{S}^2$  are symmetric with respect to the origin, it is sufficient to investigate the flow of  $p(\mathcal{X})$  only in the closed northern hemisphere. In order to draw the phase portrait on  $\mathbb{D}$ , it is necessary to project the phase portrait of  $p(\mathcal{X})$  on the northern hemisphere of  $\mathbb{S}^2$  by  $\pi$ . The points  $(u, 0)$  are the points at infinity in the local charts  $U_i$  and  $V_i$  for  $i = 1, 2$ . Additionally, we note that studying the infinite singularities only requires examining them on the local chart  $U_1$ , and determining whether the origin of the local chart  $U_2$  is or not a singularity.

## Appendix B. Topological Equivalence of Two Polynomial Vector Fields

Two vector fields  $\mathcal{X}_1$  and  $\mathcal{X}_2$  on  $\mathbb{R}^2$  are *topologically equivalent* if there exists a homeomorphism on the Poincaré disc  $\mathbb{D}$  preserving the infinity  $\mathbb{S}^1$  and taking orbits of the flow induced by  $\pi(p(\mathcal{X}_1))$  to orbits of the flow induced by  $\pi(p(\mathcal{X}_2))$ . Furthermore this homeomorphism must preserves or reverse the sense of all the orbits.

A *separatrix* of the Poincaré compactification  $\mathbb{D}$  is one of the following orbits: all the orbits at infinity  $\mathbb{S}^1$ , the limit cycles, the finite singular points, and the two

separatrices of the hyperbolic sectors of the finite and infinite equilibrium points, see [7] and [8].

Let  $\Sigma_{\mathcal{X}}$  be the set of all separatrices of the flow defined by the compactification vector field  $p(\mathcal{X})$  in the Poincaré disc  $\mathbb{D}$ . It is satisfied that  $\Sigma_{\mathcal{X}}$  is a closed set of  $\mathbb{D}$ , see [8]. Every connected component of  $\mathbb{D} \setminus \Sigma_{\mathcal{X}}$  is a *canonical region* of flow defined in the Poincaré disc.

The following theorem, independently established by Markus [7], Neumann [8], and Peixoto [9], provides the classification of phase portraits in the Poincaré disc of a planar polynomial differential system with finitely many separatrices, it suffices to describe their separatrix configuration and identify an orbit within each canonical region.

**Theorem B.1** *Let  $(\mathbb{D}, \phi)$  and  $(\mathbb{D}, \tilde{\phi})$  be two compactified Poincaré flows with finitely many separatrices coming from two polynomial vector fields. Then they are topologically equivalent if and only if their separatrix configurations are topologically equivalent.*

## Appendix C. Vertical Blow Ups

Consider a real planar polynomial differential system given by

$$\dot{x} = P(x, y) = P_n(x, y) + \dots, \quad \dot{y} = Q(x, y) = Q_n(x, y) + \dots, \quad (\text{C.1})$$

with  $P$  and  $Q$  being coprime polynomials,  $P_n$  and  $Q_n$  being homogeneous polynomials of degree  $n \in \mathbb{N}$  and the dots representing higher order terms in  $x$  and  $y$ . Since  $n > 0$ , the origin is an equilibrium point of system (C.1). Then the *characteristic directions* at the origin are given by the straight lines through the origin defined by the real linear factors of the homogeneous polynomial  $P_n(x, y)y - Q_n(x, y)x$ . Orbits that start or end at the origin are well known to do so tangentially to the straight lines determined by the characteristic directions. For more details on characteristic directions, see, for instance [2].

Suppose that we have an equilibrium point at the origin of coordinates, as in the differential system (C.1) and that this equilibrium is linearly zero. Then for studying its local phase portrait we will do vertical blow up's.

We define the vertical blow up in the  $y$  direction as the change of variables  $(u, v) = (x, y/x)$ . This change transforms the origin of system (C.1) in the straight line  $u = 0$ , analyzing the dynamics of the differential system in a neighborhood of this straight line we are analyzing the local phase portrait of the equilibrium point at the origin of system (C.1). But before doing a vertical blow-up in order that we do not lost information we must avoid that the direction  $x = 0$  be a characteristic direction of the origin of system (C.1). If  $x = 0$  is a characteristic direction, we do a suitable twist  $(x, y) = (u, u + \alpha v)$  with  $\alpha \neq 0$ , in order that new vertical straight line  $u = 0$  is no longer a characteristic direction.

**Acknowledgements** The authors thank to the Reviewers for their valuable comments and suggestions. The first author is partially supported by PEAPDI 2024 grant, CBI-UAMI. The second author is partially

supported by the Agencia Estatal de Investigación grant PID2022-136613NB-I00, AGAUR (Generalitat de Catalunya) grant 2021SGR00113, and by the Reial Acadèmia de Ciències i Arts de Barcelona.

**Author Contributions** Martha Alvarez-Ramirez and Jaume Llibre contributed to the conceptualization, methodology, and writing of the original draft, as well as reviewing the manuscript.

**Funding** Open access funding provided by Universidad Autonoma Metropolitana (BIDIUAM)

**Data Availability** No datasets were generated or analysed during the current study.

## Declarations

**Conflict of interest** The authors declare no competing interests.

**Open Access** This article is licensed under a Creative Commons Attribution 4.0 International License, which permits use, sharing, adaptation, distribution and reproduction in any medium or format, as long as you give appropriate credit to the original author(s) and the source, provide a link to the Creative Commons licence, and indicate if changes were made. The images or other third party material in this article are included in the article's Creative Commons licence, unless indicated otherwise in a credit line to the material. If material is not included in the article's Creative Commons licence and your intended use is not permitted by statutory regulation or exceeds the permitted use, you will need to obtain permission directly from the copyright holder. To view a copy of this licence, visit <http://creativecommons.org/licenses/by/4.0/>.

## References

1. Álvarez, M.J., Ferragut, A., Jarque, X.: A survey on the blow up technique. *Int. J. Bifur. Chaos Appl. Sci. Eng.* **21**(11), 3103–3118 (2011). <https://doi.org/10.1142/S0218127411030416>
2. Andronov, A.A., Leontovich, E.A., Gordon, I.I., Mañer, A.G.: *Qualitative theory of second-order dynamic systems*. Halsted Press [John Wiley & Sons], New York-Toronto; Israel Program for Scientific Translations, Jerusalem-London (1973). Translated from the Russian by D. Louvish
3. Cardo, A., Francescutto, A., Nabergoj, R.: Ultraharmonics and subharmonics in the rolling motion of a ship: Steady-state solution. *Int. Shipbuild. Prog.* **28**(326), 234–251 (1981). <https://doi.org/10.3233/ISP-1981-2832602>
4. Dumortier, F., Llibre, J., Artés, J.C.: *Qualitative theory of planar differential systems*. Universitext. Springer-Verlag, Berlin (2006)
5. Khan, N., Sulaiman, M., Tavera Romero, C.A., Laouini, G., Alshammari, F.S.: Study of rolling motion of ships in random beam seas with nonlinear restoring moment and damping effects using neuroevolutionary technique. *Materials (Basel)* **15**(2), 674 (2022). <https://doi.org/10.3390/ma15020674>
6. Llibre, J., Pantazi, C.: Global phase portraits of the quadratic systems having a singular and irreducible invariant curve of degree 3. *Int. J. Bifur. Chaos Appl. Sci. Eng.* **33**(1), 2350003 (2023). <https://doi.org/10.1142/S0218127423500037>
7. Markus, L.: Global structure of ordinary differential equations in the plane. *Trans. Amer. Math. Soc.* **76**, 127–148 (1954). <https://doi.org/10.2307/1990747>
8. Neumann, D.A.: Classification of continuous flows on 2-manifolds. *Proc. Amer. Math. Soc.* **48**, 73–81 (1975). <https://doi.org/10.2307/2040695>
9. Peixoto, M.M.: On the classification of flows on 2-manifolds. In: *Dynamical systems (Proc. Sympos., Univ. Bahia, Salvador, 1971)*, pp. 389–419. Academic Press, New York-London (1973)
10. Selvi, M., Rajendran, L., Abukhaled, M.: Estimation of rolling motion of ship in random beam seas by efficient analytical and numerical approaches. *J. Marine. Sci. Appl.* **20**, 55–66 (2021). <https://doi.org/10.1007/s11804-020-00183-x>

**Publisher's Note** Springer Nature remains neutral with regard to jurisdictional claims in published maps and institutional affiliations.